UDC 662.7:662.767:66.097
DOI: 10.15587/1729-4061.2026.352281

SYNGAS QUALITY IMPROVEMENT IN CORNCOB UPDRAFT GASIFICATION USING CAO/ACTIVATED CARBON PALM FIBER CATALYST

Purbo Suwandono
Corresponding author
Master*
E-mail: purbo@widyagama.ac.id
ORCID: https://orcid.org/0000-0003-4085-1291
Widya Wijayanti
PhD**
ORCID: https://orcid.org/0000-0003-4215-5943
Nova Risdiyanto Ismail
PhD*
ORCID: https://orcid.org/0000-0001-8439-6919
Dzulfikar Johan Akbar
Master Student**
ORCID: https://orcid.org/0009-0002-4652-8516
Muhammad Reza
Bachelor Student*
ORCID: https://orcid.org/0009-0009-9258-0586
*Department of Mechanical Engineering
Widya Gama University
Borobudur str., 35, Malang, Indonesia, 65142
**Department of Mechanical Engineering
Brawijaya University
Veteran str., 10-11, Malang, Indonesia, 65145

The object of the study is updraft fixed-bed gasification process of corncob biomass with dual catalytic system calcium oxide (CaO) and palm-fiber-derived activated carbon (AC-PF). This study addresses the low heating value of corn cob syngas and the high cost of upgrading catalysts. This study using dual catalyst system characterization along with both equivalence ratio (0.2, 0.25, 0.3, and 0.35), catalyst loading (4%, 6%, 8% and 10%) and finally CaO/AC–PF mass ratio (0:1, 1:0, 1:1, 2:1), in addition to this the final products obtained were analyzed for dual catalyst systems further through Scanning Electron Microscope, Fourier Transform Infrared Spectroscopy and Brunauer-Emmett-Teller. These results indicate that by increasing the ER, H2 and CH4 fractions increase, whereas CO_2 decreases, and the lower heating value of syngas increases, however CO reaches an optimum at ER = 0.3. Higher catalyst loading tends to decrease H_2 and CH_4 but increase CO, which potentially lowers the heating value at high loadings. Characterization of the catalyst shows that AC-PF has a porous structure and greater gas-solid contact with enhanced secondary reactions while addition of CaO creates a composite with surface species associated with CO_2 sorption. Low Heating Value of syngas rises at high ER while decreases with the increase in catalyst loadings due to the minimal contribution of CH_4. Our obtained results feature the demonstrated functional synergetic mechanism between porous AC–PF and CaO-based CO_2 sorption, allowing simultaneous catalytic upgrading and CO_2 capture in one cheap dual catalyst system. Such empirical observations would provide an appropriate foundation for future potential designs and operation of small-scale biomass gasification units, specifically updraft reactors to convert corn cob waste at the ER and catalyst loadings investigated in this study

Keywords: gasification, updraft, corncob, syngas, CaO, activated carbon

Received 20.01.2026
Received in revised form 25.03.2026
Accepted date 03.04.2026
Published date 30.04.2026

How to Cite: *Suwandono, P., Wijayanti, W., Ismail, N. R., Akbar, D. J., Reza, M. (2026). Syngas quality improvement in corncob updraft gasification using CaO/activated carbon palm fiber catalyst. Eastern-European Journal of Enterprise Technologies, 2 (6 (140)), 36–50. https://doi.org/10.15587/1729-4061.2026.352281*

1. Introduction

In recent years, with several environmental challenges such as increased greenhouse gas emissions, depletion of fossil fuels and agricultural waste, the global movement towards green energy and sustainable technologies has taken full steam. Because these issues involve not only factors that degrade environmental quality but also ones that threaten long-term energy security and sustainable economic development, they are critical subjects of concern. This is not just about cutting emissions developing green energy means finding new, cleaner, more effective methods of using what we have and generating less waste. The conversion of biomass residues into energy seems a viable and ecologically acceptable option. Gasification of biomass to get synthesis gas is one of such potential techniques which can convert solid biomass into syngas or be further transformed as feedstock for manufacturing chemicals and other energy goods.

Indonesia is among the largest corn producers in Southeast Asia, with national production exceeding more than 18 million tons of dry seed per year. About 15–20% of this amount refers to cobs after the kernel removal process, which thus leads to an excessive volume of corn cob waste (around 2.5–3.5 million tons per year). Previously, corn cobs alone

were largely underutilized and could be used for traditional Fuel as well as small quantities of Animal Feed or even burnt on post-harvest land that can lead to Air Pollution. Most are just left in heaps or to rot on the land, a potential source of plant disease [1].

Chemical and energy properties of corn cobs are quite promising. They are mainly composed of cellulose, hemicellulose and lignin, with a calorific value starting from approximately 15–17 MJ/kg, which makes them highly appropriate as initial feedstock for many biomass-based energy conversion technologies [2]. Their hardness and fibrous nature make them ideal candidates for production of biochar or activated charcoal process, or direct use in pyrolysis & gasification processes. This enormous potential shows that corn cobs are not waste, but rather a renewable resource that can be potentially leveraged for energy security and reduced fossil fuel dependence.

Biomass gasification is a promising thermochemical process to convert renewable resources into syngas containing H_2, CO, CH_4, and CO_2. Corn cobs are among the most abundant biomass types in Indonesia [3] and have a high content of lignocellulose that supports energy conversion. Nevertheless, the biomass gasification process still encounters various challenges, most notably the low hydrogen fraction of syngas and the generation of substantial amounts of tar. Tar formation can lead to clogging of the reactor, loss of thermal efficiency and high purification costs.

To address such issues, an important strategy is the implementation of catalysts. Several studies have shown that metal catalysts like Ni, Ca and K are able to enhance hydrogen yield but at the same time suppress tar formation. On the other side, enhanced carbon also widely used as catalyst support owing to high surface area, porous structure and good chemical stability. This type of biomass can be used to produce activated carbon from waste plantations that provide other socioeconomic benefits as an alternative source of raw material and is an economically viable process where the use of these resources in a circular economy opens up new potential such that palm fiber waste can be converted into valuable products. Furthermore, calcium oxide (CaO) acts both as a catalyst in the tar decomposition reaction and an absorber of CO_2 that triggers sorption-enhanced gasification to enhance hydrogen content in syngas [4].

While a lot of research has been done on metal catalysts and activated carbon, studies involving biomass bases catalyst like palm fiber-based activated carbon with CaO during the gasification of corn cob remain sparse. One originality of this study is on the use of a dual catalysts that gives a synergistic effect: high-pore activated carbon enhances both catalysts heterogeneous distribution and activity while the CaO helped to decompose tars as well as absorb CO_2. This strategy could lead to major increases in hydrogen production and decreases in carbon emissions.

The importance of improving syngas quality in biomass gasification systems has been the subject of significant scientific interest in contemporary energy studies, particularly as society confronts escalating expectations for clean, renewable, sustainable energy systems. Particular focus should be placed on these strategies aiming to increase hydrogen production and decrease tar generation, as they are still two of the main technology barriers preventing the broader practical application of biomass gasification. This makes the discovery and assessment of effective, low-cost and sustainable catalytic materials scientifically significant for the establishment of wide-ranging, efficient biomass conversion technologies to underpin transitioning from fossil-based fuels to cleaner energy use.

2. Literature review and problem statement

The paper [5] presents the result on the gasification of sago dreg waste pellets in a top-lit updraft fixed-bed gasifier. The results show that the addition of Al_2O_3 improved syngas quality, especially by increasing H_2 content up to 31.65% at 5% Al_2O_3 and enhancing CO and CH_4 production, while also increasing the H_2/CO ratio to 1.65 and 1.51 for 5% and 10% Al_2O_3, respectively, improving LHV, and reducing tar content by about 25–27.5% compared with pellets without catalyst. However, this study is limited because it was conducted only on one biomass type, within a laboratory-scale TULD fixed-bed gasifier, and only considered two catalyst loadings.

The paper [6] presents the result on hydrogen enrichment in product gas from a pilot-scale rice husk updraft gasification. The results show that dolomite-assisted air gasification gave the best performance, increasing the H_2 content up to 15.4 mol%, with an LHV of 5.1 MJ/Nm^3, while steam/air gasification improved H_2 to 9.6 mol% and air alone produced only about 7.08 mol% H_2, the optimum operating condition was reported at an airflow rate of 3 m^3/h and a dolomite mixing ratio of 15 wt.%. However, this study is limited because it focused only on rice husk feedstock, used a pilot-scale updraft gasifier with a batch capacity of 3 kg, and evaluated only a limited range of operating conditions and catalyst type.

The paper [7] presents the result on oxygen updraft gasification coupled with catalytic steam reforming of cigarette butts for hydrogen-rich syngas production. The results show that the integrated process was effective in converting cigarette butts into syngas, with gasification producing 82.3–89.7 wt.% syngas, 6.3–8.6 wt.% soot, and 1.4–1.9 wt.% tar, while the catalytic reforming stage significantly improved the gas quality by increasing the H_2 content up to 30.27 vol.%, increasing the HHV up to 11,528 kJ/kg, and reducing tar concentration from about 18.15 g/m^3 to 13.38 g/m^3 under the optimum condition. However, this study is limited because it investigated only cigarette butt waste as feedstock, used a specific oxygen updraft gasifier-catalytic reformer configuration, and fixed most catalytic reforming parameters.

The paper [8] presents the result on the experimental assessment of pellets produced from beekeeping waste and slumgum–pine sawdust mixtures through updraft gasification. The results show that pure slumgum pellets exhibited very high mechanical durability (99.98%) and high HHV (27.66 MJ/kg), while during gasification the 50% slumgum-50% sawdust pellets produced the highest producer gas LHV of 7.62 MJ/Nm^3, indicating that the addition of sawdust improved gas quality and energy recovery potential. However, this study is limited because the equivalence ratio remained very low (0.0125–0.0204) compared with typical gasification conditions, the experiments were conducted only in a modified laboratory-scale updraft gasifier.

The paper [9] presents the result on a comparative investigation of catalyst applications in updraft and modifiable-downdraft fixed-bed biomass gasifiers, using a biomass mixture of green waste, sewage sludge, and olive pomace together with red mud (RM) and Al-Ni alloy catalysts to im-

prove syngas quality and hydrogen production. The results show that catalyst type and reactor configuration strongly influenced gasification performance, with the Al-Ni catalyst giving the best hydrogen enrichment, reaching up to 65 vol.% H_2 in the updraft gasifier at 900°C, while RM increased H_2 to about 50 vol.%, the updraft gasifier produced better hydrogen-rich syngas than the modifiable-downdraft reactor. However, this study is limited because it, used a specific mixed biomass composition and mainly focused on high temperature operation around 900°C with limited gasifying-agent flow conditions.

The paper [10] presents the result on the experimental investigation of producer gas composition from sorted municipal solid wastes in an updraft fixed-bed gasifier. The results show that reducing the equivalence ratio from 0.21 to 0.15 increased the heating value of the combustible gases. The study indicated that the allothermal updraft fixed-bed gasifier is suitable for producing gas that can be utilized in gas engines. However, this study is limited because it used a laboratory-scale 10 kW allothermal updraft gasifier at a fixed temperature of 800°C, and evaluated only two ER conditions.

The paper [11] presents the result on the effect of adding laying hens' manure (LHM) to wheat straw on gasification efficiency in an air-blown updraft fixed-bed gasifier. The results show that increasing ER improved the gasification performance, with the producer gas LHV reaching 3.3–3.4 MJ/m^3, cold gas efficiency around 60%, and carbon conversion efficiency in the range of 82–94%. However, this study is limited because it was focused on one specific co-feed system and produced a relatively low-calorific gas.

The paper [12] presents the result on the gasification performance of olive pomace in updraft and downdraft fixed-bed reactors using dry air and pure oxygen. The results show that updraft reactor achieving up to 48 vol.% H_2 with dry air and 53 vol.% H_2 with pure oxygen, while the downdraft reactor reached up to 45 vol.% H_2 with dry air and 39 vol.% H_2 with pure oxygen. However, this study is limited because only a limited range of gasifying agents, temperatures, and flow rates.

The paper [13] presents the result on the gasification of MDF residue in an industrial-scale updraft fixed-bed gasifier. The results show that MDF residue can be effectively converted into useful energy, with a syngas production rate of about 2.5 Nm^3/kg, syngas LHV of around 6.0–7.0 MJ/Nm^3, about 88 wt.% of MDF residue converted into syngas, and a system capable of delivering 7 MWth of thermal energy and about 955 kW net electrical power through the ORC turbine. Nevertheless, this study is subject to some limitations as it investigated only a single industrial waste stream (corn cob) in a single updraft gasifier design and performance was assessed with few feed rates while direct combustion of raw hot syngas containing tar was employed.

This study shows the outcomes of researches conducted on updraft fixed-bed reactors with biomass gasification concerning improvement of syngas quality and efficiency of thermal conversion. Demonstrated that syngas composition and heating value are significantly impacted by feedstock properties, gasification conditions, and catalysts. However, problems associated with the absence of high-performance and inexpensive catalyst systems that can boost hydrogen generation in addition to optimizing syngas quality simultaneously during corncob gasification were not solved. This is due to the intricacy of catalytic processes occurring in the gasification area along with reforming, cracking and CO_2 capture pathways along with financial restrictions of promoted catalyst existing available on a market. Perhaps utilizing coupled composite catalysts consisting of CaO and activated carbon palm fiber proves to be a solution for these concerns, wherein the CaO stimulates CO_2 uptake and drives shift reactions while Coconut shell active carbon provides a porous surface and serves as an external site for secondary cracking reactions. It has been used in prior studies, but the application of CaO and activated carbon palm fiber for corncob updraft gasification is still limited. It can be concluded that a syngas quality improvement study on corncob updraft gasification using CaO/activated carbon palm fiber catalyst is recommended.

Biomass gasification represents a significant path for transforming agricultural remains into useable synthesis gas, and catalytic materials (e.g., CaO and carbonaceous adsorbents) has been shown to enhance the quality of produced gases via tar decomposition, reforming reactions, and CO_2 capture. A number of researchers have studied other biomass feedstocks, catalyst type and reactor configurations for improving syngas production. Nevertheless, most of these studies were mainly on the single performance of catalysts or gasification systems other than corncob updraft gasification. Moreover, the synergistic effect of CaO and activated carbon palm fiber catalyst with respect to catalyst dosage ratio, catalyst loading and equivalence ratios remained largely undocumented.

Thus, additional research is important for evaluating the synergism of CaO as a CO_2 sorbent and activated carbon palm fiber as a porous catalytic support in improving syngas composition and heating value. In view of this research gap, the current study aims to explore the role of combined CaO/activated carbon palm fiber catalyst in corncob updraft gasification along with the effects of different operating parameters on synthesis gas quality. Thus, this study is meant to deliver a more clear scientific angle of catalyst interaction and practical directions for performance enhancement in biomass gasification.

3. The aim and objectives of the study

The aim of this study was to improve syngas quality from corncob updraft gasification via a dual-synergy catalytic system composed of calcium oxide (CaO) and palm-fiber-derived activated carbon (AC-PF). This will enable cleaner and more energy-dense producer gas production, offering practical guidance on the utilization of operating conditions and catalyst configurations applicable to updraft gasification of agricultural residues.

To accomplish these aims, the following objectives are achieved:

– to prepare and characterize CaO and AC-PF catalysts by analyzing their morphology, surface functional groups, and pore characteristics using SEM, FTIR, and BET methods;

– to determine the effect of the equivalence ratio, catalyst loading and CaO/AC ratio on the composition of syngas and its lower heating value in updraft gasification of corncobs and to obtain the catalyst condition responsible for higher quality gas.

4. Materials and methods

4. 1. The object and hypothesis of the study

It is based on the updraft fixed-bed gasification process of corncob biomass at dual calcium oxide (CaO) and palm-fiber-derived activated carbon (AC-PF) catalyst systems, which

are used for the purpose of study. Experimental parameters adopted in the updraft reactor studying catalytic upgrading of producer gas were expected to affect syngas composition and heating value. The focus of this study is to develop a method for applying its results in order to enhance the quality syngas by increasing the flammable fraction of combustible gases (H_2 and CH_4) and lower heating value (LHV); while reducing CO_2 concentration at the same time.

This study hypothesizes that the dual-synergy CaO/AC-PF catalytic system is a more positive effect on syngas quality in comparison with single-catalytic configurations during updraft corncob gasification. The hypothesis is that CaO acts as a CO_2 sorbent, driving the equilibria of reactions to yield more hydrogen while palm fiber-derived activated carbon provides high surface area catalytic sites, facilitating secondary kinetics like tar cracking and volatile reforming. Optimized conditions of equivalence ratio (ER), catalyst loading, and CaO/AC-PF ratio are expected to not only increase H_2 and CH_4 fractions but also enhance LHV due to the effects of a combined catalytic-sorption mechanism.

It was defined that the corncob feedstock had relatively homogeneous composition and stable proximate/ultimate characteristics through the duration of experiments. It was assumed that after stabilization, the gasification process ran under steady-state conditions. It is also assumed that the CaO has enough CO_2 sorption capacity for the duration of catalytic conversion process and activated carbon structure was stable within applied temperature range.

Several methodological simplifications were applied throughout the research to enable experimental feasibility and focus on the goal of syngas quality evaluation. Detailed kinetic modeling of individual gasification reactions was not carried out but rather based the process performance on experimentally measured syngas composition and syngas low heating value. Moreover, although carbonation-decarbonation reactions of CaO can take place during operation, the microstructural evolution, sintering behavior and long-term cyclic stability of the catalyst were not studied in this work. the catalytic performance was assessed over the experimental time period with no prolonged durability or regeneration-cycle assessment.

The selected methods were intended to explain both the catalyst characteristics and their effect on syngas quality. SEM, FTIR, and BET were used because they provide complementary information on catalyst morphology, surface functional groups, and pore structure, which are important for catalytic reforming, adsorption, and CO_2 capture during gasification. The investigated operating parameters, namely equivalence ratio, catalyst loading, and CaO/AC ratio, were chosen because they are the main variables governing the reaction environment, catalyst effectiveness, and synergistic interaction between CaO and activated carbon in the updraft gasification process.

4. 2. Catalyst preparation

Approximately 6 grams of ground palm fiber was mixed with 60 mL of distilled water and stirred for 10 minutes. The mixture was then placed in an autoclave and heated to 200°C at a rate of 5°C per minute for 6 hours in an electric oven. After that, the reactor is allowed to cool naturally to room temperature. The resulting solid hydrocarbon product (hydrochar) is then separated using Whatman No. 42 filter paper. The filtered product is then dried at 105°C for 24 hours and stored in a glass vial. The next stage is the activation process. The hydrochar is immersed in a 3 M KOH solution with a weight ratio of 1:3 (Hydrochar:KOH) for 16 hours, then dried at 85°C for 6 hours. Spectroscopic evidence indicates that KOH preferentially reacts with oxygenated sites and can increase the relative abundance of C–OH functionalities, while higher KOH ratio and activation temperature significantly enhance porosity and BET surface area [14, 15]. To obtain the CaO/AC mixture, CaO powder and activated carbon (AC) were mixed in specific proportions using a grinder until a homogeneous mixture was obtained. Next, CaO, AC, and CaO/AC were activated using a tube furnace at a temperature of 700°C for 1 hour with a continuous flow of nitrogen during the activation process. The resulting product was then washed using distilled water until it reached a neutral pH. This stage produced activated carbon that was ready for use in research.

4. 3. Experimental setup

Corncob biomass was obtained from farmers in the South Malang region of East Java. Before use, the biomass was cleaned of impurities and dried in an oven for 6 hours at 100°C to remove moisture (water vapor) content. The ultimate and proximate test results are as follows.

The proximate and ultimate analyses of the corncob feedstock were conducted to determine its physicochemical characteristics prior to gasification. The results are presented in Table 1. The data indicate that corncob has high volatile matter content and relatively low ash content, which are favorable characteristics for gasification processes.

Table 1

Ultimate and proximate test corn cob

Parameter	Units	Corn cobs
Moisture	%	10
Volatile matter	%	71.38
Fixed carbon	%	12.11
Ash	%	6.51
C	%	43.6
H	%	6.3
O	%	46.8
N	%	0.22
HHV	MJ/kg	17.61

The experimental apparatus employed in this study consisted of an updraft gasifier integrated with a catalyst bed, a vapor condensation unit, gas sensors, and temperature measurement points to enable comprehensive monitoring of the gasification process. Fig. 1 shows the updraft gasifier system used in this study, including the schematic experiment (*a*) and the experimental setup (*b*).

This study used an updraft gasification reactor designed with a total height of 20 cm. The lower part of the reactor consisted of an ash container with a height of 5 cm, while the active reactor had a height of 15 cm and a diameter of 3 inches. The reactor was equipped with a 1-inch diameter air inlet pipe connected to a blower. The blower was modified with a potentiometer so that the air speed could be adjusted as needed. To monitor the thermal conditions inside the reactor, four 3 cm long type K thermocouples were installed at several different points so that the temperature profile in the gasification zone could be observed in more detail. Each test was conducted with a fixed biomass mass, a mixture of corn cobs weighing 80 grams. The reactor was made of iron and equipped with a gas seal to prevent leaks during the gasification process.

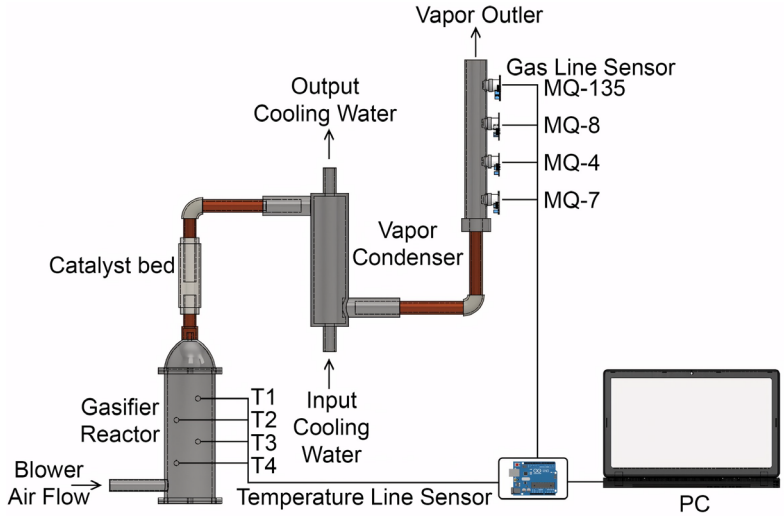

a

b

Fig. 1. Updraft gasifier: *a* — schematic experiment; *b* — experimental setup

The gas produced by the reactor was fed into a condenser, which cooled the hot gas so that the water vapor components could be separated. The condenser was made of a copper spiral pipe with a diameter of ½ inch and a height of 30 cm. Cooling water was circulated from the bottom of the condenser and exited through the top to ensure efficient heat transfer. This cooling system was driven by a 60-watt water pump, ensuring stable water flow and optimal condensation. The catalyst was positioned downstream after the reactor, where it was supported on steel wool and wrapped with an 80-μm wire mesh to secure the catalyst and prevent particle carryover with the gas flow.

To analyze the gas composition, four types of MQ gas sensors were used. The MQ-8 sensor was used to detect H_2, MQ-4 for CH_4, MQ-135 for CO_2 and MQ-7 for CO. Each gas sensor was calibrated according to the manufacturer's datasheet, specifically by determining the Ro value, which is the sensor resistance in clean air conditions. This Ro value is used as a reference in calculating the measured gas concentration during the process.

All data from the gas sensors and thermocouples were acquired using an Arduino Uno microcontroller. Each gas sensor is connected to a separate Arduino Uno to facilitate the calibration process and reduce the possibility of interference between sensors. Arduino is also used to record temperature data from four thermocouples installed in the reactor, so that gas composition and temperature distribution data can be obtained simultaneously.

The ER range of 0.2, 0.25, 0.3 and 0.35. The catalyst load was between 4%, 6%, 8% and 10% from the mass of input feedstock. The CaO/AC-PF ratio was varied between 0:1, 1:0, 1:1, and 2:1. Design of experiment can be seen in Table 2.

Table 2

Design of experiment using

Run	Equivalence ratio (E.R)	Catalyst load, %	CaO/AC
1	0.2	4	1:0
2	0.2	6	0:1
3	0.2	8	1:1
4	0.2	10	2:1
5	0.25	4	0:1
6	0.25	6	1:0
7	0.25	8	2:1
8	0.25	10	1:1
9	0.3	4	1:1
10	0.3	6	2:1
11	0.3	8	1:0
12	0.3	10	0:1
13	0.35	4	2:1
14	0.35	6	1:1
15	0.35	8	0:1
16	0.35	10	1:0

A total of 16 experimental runs were conducted systematically to enable evaluation of the main effects of each variable and the tendency of interactions between variables on the fractions of H_2, CO, CH_4, CO_2, and lower heating value (LHV). This approach enabled identification of the most effective combination of operating parameters in improving syngas quality quantitatively and measurably.

5. Results of syngas quality enhancement from corncob using calcium oxide (CaO) and palm-fiber-derived activated carbon (AC-PF).

5. 1. Characterization of calcium oxide (CaO) and palm-fiber-derived activated carbon (AC-PF) catalysts

5. 1. 1. Scanning electron microscopy catalyst result

Fig. 2, *a* indicates the surface morphology of palm fiber-based activated carbon (AC-PF). The close look at the surface reveals a porous and non-plane structure with void sections surrounded by massive stack surfaces. This property shows that the activation of KOH has successfully created micropores and mesopores, which are crucial in enhancing activated carbon specific surface area.

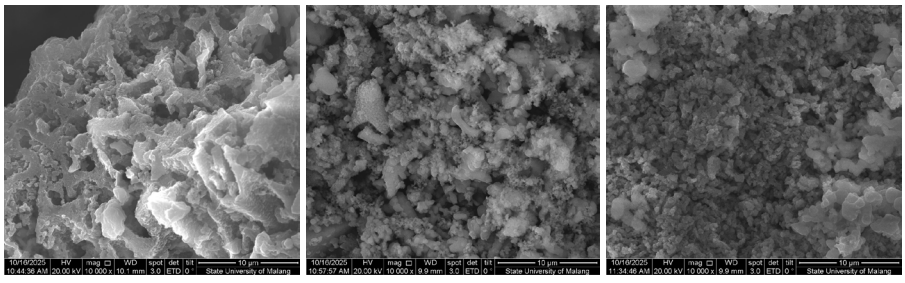

a *b* *c*

Fig. 2. Scanning electron microscopy catalyst result:
a — scanning electron microscopy AC-PF; *b* — scanning electron microscopy CaO:AC, 1:1;
c — scanning electron microscopy CaO:AC-PF, 2:1

This the coarse and textural surface shows that most of the material has been exposed from lignocellulose cell wall, which had many interparticle voids. When serving as a catalyst in gasification or thermochemical reactions, this porous architecture significantly promotes the ability of an adsorbed dispersed gas to diffuse on and into the structure.

The small size of the voids (1–5 μm) indicates that most of the pores belong in the mesopores category where gas molecules such as H_2, CO and tar can attach during a gasification reaction.

The porosity and aspect of AC-PF exhibit the properties of porous activated carbon materials with a heterogeneous pore structure, where pores facilitate interaction between gas phase reactants and active sites surrounding each other on the surface area of materials which increases reaction rates and improved tar or CO_2 capture targeting in biomass-derived power applications.

Fig. 2, *b* represent the surface morphology of CaO:AC-PF catalyst in 1:1. The approach of this material surface can be observed, composed of fine particles with microns and submicrons that bond together to build a layered and slightly agglomerate system.

Fine and light-colored grains suggest a well-distributed CaO particle, doped on the surface of activated carbon (AC-PF). This distribution of CaO through the pores fills some of them creating a particle with a denser surface than that observed pure AC-PF. Nevertheless, small gaps and tiny voids between the grains still point to preserved microporous and mesoporous configurations that can indeed support catalytic activity [16].

Such morphology shows the effectiveness of the CaO impregnation technique using activated carbon originated from palm fiber, where interactions between CaO and pore walls of carbon formed a composite material that provides greater thermal stability and chemical stability. This framework is particularly well-suited for catalyst applications in biomass gasification processes, because CaO particles may act as CO_2 absorbers and also facilitate the tar reforming reaction [17].

Fig. 2, *c* displays the surface appearance of CaO:AC-PF (2:1) catalyst. This implies that the exposed material is covered in agglomerations of fine, round and irregular particles between microns to submicrons. These results prove that, in comparison with CaO:AC-PF (1:1) sample, its structure becomes denser and much tighter, meaning that the increase in the ratio of CaO will lead to a partial closure effect of activated carbon surface pore by CaO particles.

In fact, the CaO particles are more evenly distributed and fill the carbon surface, which proves that there is a greater amount of CaO being successfully impregnated. Notably, the light color in certain regions suggests a calcium oxide phase that is well adhered to the activated carbon matrix. Such structure suggests the strong bonding interactions between CaO and AC-PF forming a high temperature stable composite.

While some of the pores are blocked, small voids between the CaO grains still exist where gas can diffuse, and therefore the adsorption ability of catalyst remains large. Due to the active area of CaO and porous carbon structure, this material is very competitive in biomass gasification or tar reforming applications since CaO can be CO_2 absorber and enhance conversion of carbon into H_2,

5. 1. 2. Fourier transform infrared spectroscopy catalyst result

The FTIR analysis results shown in the Fig. 3 reveal clear spectral differences between the AC-PF, CaO, and their mixtures (CaO:AC-PF) with ratios of 2:1 and 1:1. In the AC-PF spectrum, the absorption band at 2926 cm^{-1} is associated with the stretching vibration of the C–H group from $-CH_2$ or $-CH_3$ (methylene/methyl stretching), which indicates the presence of hydrocarbon chain residues from the lignocellulose structure. The peak at 1577 cm^{-1} indicates the presence of aromatic C=C or C=O stretching, while the band at 1056 cm^{-1} represents C–O stretching from alcohol or ether groups. In addition, the -OH group that appears in the 3500–3600 cm^{-1} region is identified as the result of AC-PF activation using a KOH solution, which causes the formation of hydroxyl groups on the activated carbon surface. This –OH group plays an important role in increasing the surface activity and adsorption capacity of AC-PF as a catalyst support medium [18, 19].

In pure CaO, the intense band at 3639 cm^{-1} is associated with the stretching of the O-H group from $Ca(OH)_2$, which is formed due to the partial hydration of CaO when exposed to humid air. Meanwhile, the absorption bands at 1426 cm^{-1} and 876 cm^{-1} are associated with C-O stretching and CO_3^{2-} bending, respectively, indicating the formation of $CaCO_3$ due to CO_2 adsorption from the air. This shows that CaO is highly reactive to moisture and carbon dioxide in the environment.

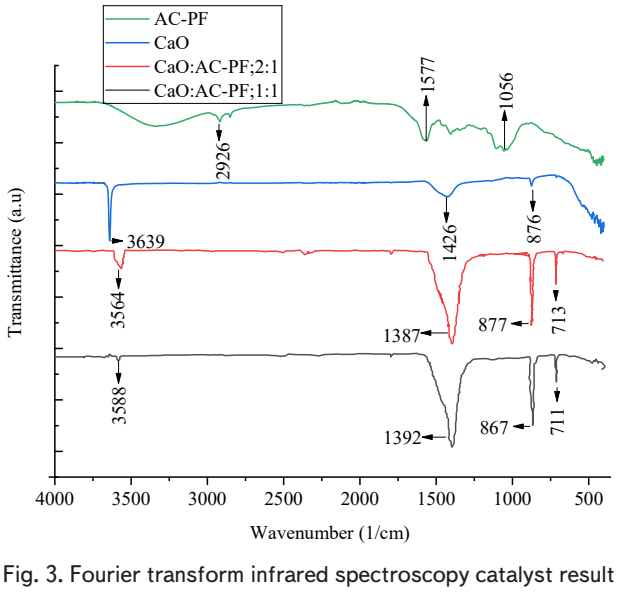

Fig. 3. Fourier transform infrared spectroscopy catalyst result

For the CaO:AC-PF (2:1), the main absorption bands were detected at 3564 cm^{-1} (O-H stretching from $Ca(OH)_2$ and the -OH group in AC-PF), 1387 cm^{-1} (C-O stretching), and 877 cm^{-1} and 713 cm^{-1} (bending vibration of CO_3^{2-}). This combination of bands indicates the formation of carbonate compounds ($CaCO_3$) due to the interaction between CaO and the oxygen groups of activated carbon. The presence of -OH groups from KOH activation also strengthens the basic properties on the surface, which can increase the chemical interaction between CaO and AC-PF [20].

At a CaO:AC-PF ratio of 1:1, the absorption bands at 3588 cm^{-1}, 1392 cm^{-1}, 867 cm^{-1}, and 711 cm^{-1} show a similar pattern, indicating the presence of hydroxyl (O-H) and carbonate $\left(CO_3^{2-}\right)$ groups. The difference in peak intensity compared to the 2:1 ratio indicates variations in the level of interaction between CaO and the –OH groups resulting from KOH activation on AC-PF, which affects the formation of carbonate-hydroxide complexes on the material surface [21].

5. 1. 3. Brunauer-Emmett-Teller catalyst result

Fig. 4 shows the adsorption-desorption isotherm curves for nitrogen for the AC, CaO:AC (1:1), and CaO:AC (2:1) samples are shown in Fig. 4. All three samples exhibit type IV isotherms with clear hysteresis loops at relatively high pressures ($P/Po > 0.9$). Based on the IUPAC classification, this characteristic indicates that the material has a mesoporous structure formed through capillary condensation within the pore channels. The difference between the adsorption and desorption pathways indicates that the pore shape is not perfectly cylindrical, but rather tends to be irregular or slit-like, which is commonly found in modified activated carbon materials [22].

The pure activated carbon (AC) sample showed a relatively low nitrogen adsorption volume with a specific surface area of 24.51 m^2/g and an average pore diameter of 0.74 nm, indicating a predominance of microporous structures. In the CaO:AC (1:1) composite, the surface area did not change significantly compared to pure AC, indicating that the addition of a moderate amount of CaO did not cover the carbon pores much, but only adhered to the external surface of the carbon matrix [23].

In contrast, the CaO:AC (2:1) mixture had a prompt sharp increase in adsorption volume at higher pressure ($P/Po > 0.9$), around about 35 cm^3/g STP, while with significantly decreased BET surface area of 5.06 m^2g and increased pore diameter to 22.87 nm

These changes in both isotherm shape and pore size increase suggest that CaO impregnation not only contributes to surface chemistry modification but also leads to substantial pore structure alteration of AC. Although this transformation is helpful, regarding catalytic applications in biomass gasification processes with respect to tar reforming and water-gas shift reactions, due to the generation of mesoporous structure that improves the diffusion of gases along with better access to active sites. Therefore, while the mesoporous catalyst has a low specific surface area, its increased mesoporosity and pore interconnection are able to enhance catalytic performance in hydrogen gas production [24].

Fig. 4, *b* presents the BJH pore size distribution curves that afford more insight into the textural evolution of palm-fiber-based activated carbon subsequent to CaO impregnation. The pristine AC shows a fairly moderate *dV/dD* value and large contribution only at the larger pore diameters (> 60 nm), suggesting its pore system is predominately macropores with very little amount of mesopores. This texture is less suitable for gas-solid reactions since the surface area available in the mesopore range (2–50 nm) is relatively small.

The BJH curves exhibit a dramatic transformation in terms of their shape and intensity after loading with CaO. In the case of CaO:AC-PF = 1:1, all other things being equal, the pore size distribution is skewed towards smaller diameters and has a larger contribution in said mesopore range (approx. 15–60 nm). This behavior indicates that CaO impregnation partially reform the carbon network, increasing volume of micropores and providing access to blocked pores, thus creating additional mesoporosity. Strengthening this effect is the CaO:AC-PF = 2:1, which shows the highest *dV/dD* in its curve and a clearly defined maximum located at ~30–40 nm. The pronounced peak within this range confirms that the greater loading of CaO favors the appearance of well-defined mesopores and suppresses the relative amount of very large macropores.

Overall, the BJH analysis demonstrates that CaO acts not only as a reactive sorbent but also as a textural promoter for the palm-fiber AC. The increase in mesopore volume and the shift of the dominant pore size toward 20–40 nm are expected to facilitate the diffusion of gasifying agents and tar molecules, as well as to improve the accessibility of CaO active sites for CO_2 capture and reforming reactions. These features are therefore beneficial for enhancing the catalytic performance of the CaO/AC composite in biomass gasification toward H_2-rich syngas production.

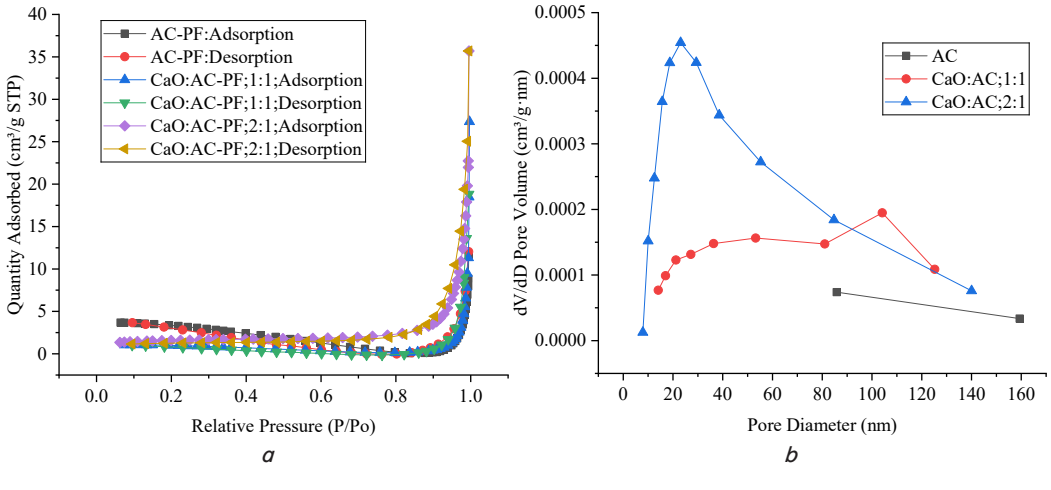

Fig. 4. Brunauer-Emmett-Teller result: *a* — surface analysis adsorption desorption isotherm; *b* — Barrett-Joyner-Halenda adsorption pore size distribution

5. 2. Effect of operating parameters on syngas composition and low heating value

5. 2. 1. Effect of equivalence ratio on syngas product

The composition of syngas from updraft gasification is greatly influenced by the equivalence ratio (ER), which is the ratio of the mass flow rate of air compared to the mass flow rate of corncob in the experiment compared to the stoichiometry of air required for complete combustion of corncob. In this study, the ER used was 0.2–0.35 with the following formula

$$ER = \frac{\left(\dot{m}_a / \dot{m}_{cc}\right)_{\exp}}{\left(\dot{m}_a / m_{cc}\right)_{stc}},$$

where $\dot{m}_a$ – the air mass flow rate (kg/s), $\dot{m}_{cc}$ – the corncob mass flow rate (kg/s), exp denotes the experimental air-fuel ratio, and *stc* denotes the stoichiometric air-fuel ratio.

The composition of syngas produced from corncob gasification was evaluated at different equivalence ratios to determine the variation in the main combustible and non-combustible gas components. Changes in the equivalence ratio significantly affected the concentrations of H_2, CH_4, CO, and CO_2, indicating that the air supply plays an important role in the gasification performance and gas quality. Fig. 5 shows the syngas composition obtained at different equivalence ratios.

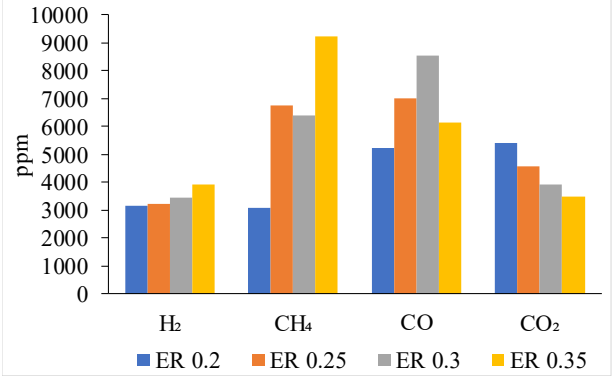

Fig. 5. Syngas composition with different equivalence ratio

The graph above shows that the higher the ER, the higher the hydrogen composition produced. At ER 0.2, the ppm is 3150 ppm, at ER 0.25 it is 3241 ppm, at ER 0.3 it is 3457 ppm, and at ER 0.35 it is 3914 ppm. A higher oxidant supply promotes the formation of more stable autothermal conditions and higher reaction temperatures due to partial oxidation. This increase in temperature accelerates hydrogen-forming reactions, particularly the gasification of active carbon catalyst interactions with steam ($C + H_2O \rightarrow CO + H_2$), the reforming of volatile compounds/light hydrocarbons ($CxHy + H_2O \rightarrow CO + H_2$), and the cracking of tar/volatile into lighter gas species. At low ER, some volatiles tend to be incompletely converted and still have the potential to escape as condensable components, while increasing ER increases heat availability, making the conversion of volatiles into gas fractions (including H_2) more effective.

The higher the ER, the higher the CH_4 composition produced. At ER 0.2, 3093 ppm was obtained, at ER 0.25 6767 ppm, ER 0.3 6377 ppm, and ER 0.35 9221 ppm. This trend indicates that the supply of oxidants not only increases autothermal conditions and the rate of devolatilization, but also shifts the reaction pathway towards the formation of light hydrocarbons through hydrogenation and/or methanation reactions in the reactor zone where the temperature still supports CH_4 formation. In particular, increased H_2 at higher ERs can promote the methanation reaction of CO ($CO + 3H_2 \rightleftharpoons CH_4 + H_2O$), so that CH_4 increases along with a tendency for CO to decrease at the highest ER. In addition, more intensive fragmentation of volatiles and tar at high ERs has the potential to produce light gas precursors which are then hydrogenated to CH_4.

CO formation increased up to an ER of 0.3 and decreased at an ER of 0.35. At an ER of 0.2, 5238 ppm was obtained, at an ER of 0.25, 6999 ppm, at an ER of 0.3, 8532 ppm, and decreased at an ER of 0.35 to 6145 ppm. At low ER (0.20–0.25), limited oxygen supply resulted in relatively low heat release, so that the reaction zone temperature and char reactivity were not sufficient to intensify CO formation reactions, especially the Boudouard reaction ($C + CO_2 \rightleftharpoons 2CO$) and char gasification with steam ($C + H_2O \rightleftharpoons CO + H_2$). When the ER is increased towards 0.30, the increase in autothermal heat strengthens these reduction reactions, causing CO formation to increase and reach its peak. However, at higher ERs (0.35), the CO fraction tends to decrease because some CO can be converted to CH_4.

CO_2 formation continues to decrease as ER increases. At ER 0.2, 5412 ppm is obtained; at ER 0.25, 4592 ppm; at ER 0.3, 3916 ppm; and at ER 0.35, 3479 ppm. The increase in oxidant supply at this ER does not promote complete combustion, but rather strengthens the CO_2 reduction mechanism. At higher ERs, the heat generated from partial oxidation increases the temperature of the reduction zone, thereby accelerating the Boudouard reaction ($C + CO_2 \rightleftharpoons 2CO$), in which CO_2 is reduced by char to CO. This mechanism is consistent with the increase in CO until it reaches a maximum at an ER of 0.30, while also explaining the decrease in CO_2 under the same conditions. Interestingly, at an ER of 0.35, CO_2 remains at its lowest level even though CO decreases, indicating that the CO formed is not completely accumulated at the outlet but has the potential to undergo further conversion along the gas flow path.

5. 2. 2. Effect of catalyst loading on syngas product

The catalyst load or amount of catalyst in this study was 4%, 6%, 8%, and 10% of the total biomass weight. Fig. 6 shows that the composition of H_2 and CH_4 increases as the catalyst load decreases. The H_2 gas composition at catalyst loads of 4%, 6%, 8%, and 10% is 3742 ppm, 3471 ppm, 3372 ppm, and 3176 ppm, respectively. As the catalyst load increases, the reaction pathways that consume H_2 tend to strengthen, particularly the reverse water–gas shift ($CO_2 + H_2 \rightarrow CO + H_2O$) and H_2 interactions on the catalyst surface during the conversion of gasification compounds. As a result, even though reforming occurs, the measured net H_2 decreases because more H_2 is used for CO formation and surface reactions. The CH_4 gas composition at catalyst loads of 4%, 6%, 8%, and 10% was 7031 ppm, 6476 ppm, 6206 ppm, and 5746 ppm, respectively. An increase in catalyst load increases the number of active sites and gas-catalyst contact, so that methane/light hydrocarbon cracking and reforming occur more intensely. CH_4 then acts as a reactant that is converted into more reactive syngas components, causing the CH_4 concentration to decrease at higher catalyst loads.

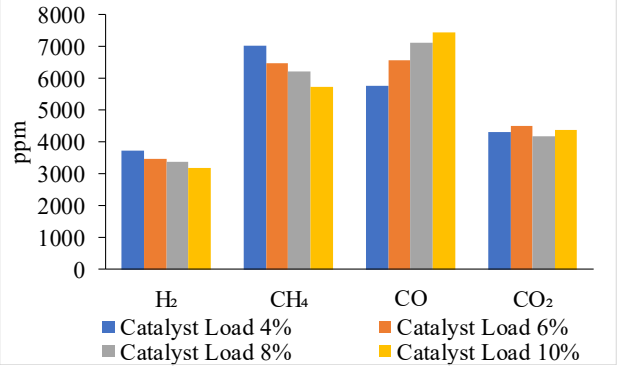

Fig. 6. Syngas composition with catalyst load variation

The CO gas composition increases with increasing catalyst load, namely for catalyst loads of 4%, 6%, 8% and 10% at 5782 ppm, 6576 ppm, 7111 ppm and 7445 ppm, respectively. The increase in catalyst loading strengthens the CO-forming reactions, particularly dry reforming ($CH_4 + CO_2 \rightarrow 2CO + 2H_2$), char – CO_2 reaction ($C + CO_2 \rightarrow 2CO$), and reverse water-gas shift. This combination shifts the product selectivity towards CO, so that the CO fraction increases consistently as the catalyst is increased. The CO_2 gas composition tends to stagnate with increasing catalyst loading, at catalyst loads of 4%, 6%, 8%, and 10% at 4322 ppm, 4510 ppm, 4198 ppm, and 4369 ppm, respectively. CO_2 shows minor changes because it is in a searching for a chemical equilibrium between the partial oxidation and the dry reforming. When the catalyst load increases, the rate of CO_2 consumption may rise, but this is often offset by CO_2 formation in the reaction zone, so that the CO_2 value appears stable or only fluctuates.

5. 2. 3. Effect of catalyst ratio on syngas product

At 4% catalyst load, the ratio of CaO/AC alters reaction thermodynamics as differences in tar cracking/reforming and CO_2 capture by CaO dominate the gasification reaction; thus, the composition of bio-gas changed significantly at mass loadings where greater amounts of active sites are available for gas diffusion to contact with the catalytic surface. At 0:1 (AC), CH_4 and CO are quite high as AC fosters volatile/tar cracking but CO_2 remains elevated due to lack of absorption. At 1:0 (CaO) CH_4 drops but the CO_2 is at its maximum, implying that there is not enough carbonate layer formation/surface area to absorb CO_2. A 1:1 ratio yields maximal CO at moderate levels of CO_2, suggesting CaO–AC synergy that enhances the conversion from volatiles to reactive gases. On the other hand, the 2:1 (CaO-rich) ratio gives the highest H_2 and lowest CO_2 due to sorption-enhanced CaO effect, but also high CH_4 because of lower contribution of AC, therefore methane reforming/cracking is still not optimal.

To explore the catalytic performance more closely, the CaO/AC ratio effects on syngas composition were carried out with multiple catalyst loading conditions. Through this study, it was aimed to investigate the effect of varying proportions of CaO and activated carbon using different catalyst loads on yield distribution of H_2, CH_4, CO and CO_2 from corncob gasification. Fig. 7 shows the influence of CaO/AC ratio at a catalyst load of 4% (*a*), 6% (*b*), 8% (*c*) and also for 10% (*d*).

Since at a catalyst loading of 4% the CaO/AC ratio alters the gasification reaction by switching between whether tar cracking/reforming is favored or CO_2 captures more CaO, it implies that under such conditions, the resultant gas composition is strongly dependent upon both number of active sites and effectiveness of contact between the gas and catalyst. Because AC promotes cracking of tar and volatile, CH_4 and CO are relatively high at 0:1 (AC); however, because no absorption occurs, the level of CO_2 remains high. By 1:0 (CaO), CH_4 is less abundant but CO_2 has reached its maximum concentration, suggesting negligible capture of CO_2 as surface area and a carbonate layer continues to grow. The high CO yield and moderate CO_2 reflect the CaO–AC synergies present in a 1:1 ratio which translate to an elevated conversion of volatiles into reactive gaseous products. On the other hand, due to the sorption-enhanced CaO effect with wider pore area presence alongside having lowest CO_2 for 2:1 (CaO-rich) ratio thus highest H_2 but CH_4 is still high alongside since lesser contribution from AC thus methane reform/cracking not ideal yet.

At a catalyst loading of 6%, CaO/AC ratio produces mainly an alteration in selectivity for secondary reactions (tar cracking/reforming and CO_2 capture) as AC favors the conversion of volatiles/light hydrocarbons, whilst CaO inhibits CO_2 via carbonate formation ($CaO + CO_2 \rightarrow CaCO_3$) and modifies reaction equilibrium. At 0:1, because there was no CO_2 capture and methane reforming is not yet optimal, volatiles escape as CH_4 while keeping high levels of CH_4 and CO_2. And so, at 1:0 CO_2 goes down most but CH_4 is lifted to highest because of the lack of AC cracking/reforming. Ideal (1:1) conditions are shown where the H_2 is maximized and CO_2 is minimized, suggesting synergies of CaO–AC leading to sorption-enhanced reforming with increasing conversion of hydrocarbons into components of a syngas. At 2:1, CO is maximized and CO_2 is minimized, but CH_4 increases again (H_2 is still not maximally usable since free circulating CaO has potential to rapidly carbonate or create contact limitations making AC a less efficient contributor for cracking/reforming).

The ratio of CaO/AC influences loss of selectivity in the syngas reaction at 8% loading. There is a high CH_4 (0:1 AC), because some light hydrocarbon are not converted even if tar cracking occurs. CO is very high at 1:0 (CaO) but CO_2 can also be very high, implying this condition favors the pathway towards CO formation along with not-so-optimal conditions for capture of increased amount of CO_2 either due to limited contact or carbonation saturation. The lowest CH_4 means that the CaO–AC synergy proved to be most effective in cracking/reforming light hydrocarbons and converting methane to reactive gas with a 1:1 rate. At 2:1, CO increases yet more but CH_4 does too; therefore, the lower AC fraction suppresses the methane reforming/cracking activity causing lower overall CO_2 concentration thus also dependent on effectiveness of CaO sorption.

At a catalyst load of 10%, the addition of total catalyst makes secondary reactions, reforming, solid-gas heterogeneous reactions and equilibrium shifts very dominant, so that product selectivity mainly depends on the ratio of CaO/AC. At 0:1 (AC), CO formation is the highest because porous carbon surfaces facilitate the cracking/reforming of volatiles and tar-to-reactive-gases conversions. The CO_2 can be retained by CaO via carbonation at ratios with CaO (1:0, 1:1, 2:1) but the effect is often encountered to be non-linear towards high loads as the CaO quickly carbonates/diffusion limits and pore blocking happen so that in conditions rich of CaO (2:1) the CH_4 arguably might decrease however CO_2 can elevate while H_2 would not be reach at full potential due reaction competition. Overall, AC-dominant promotes CO at 10% load; CaO-dominant suppresses light hydrocarbons but tempts non-ideal conditions (saturation/mass transport) that destroy the benefits of H_2 and CO_2.

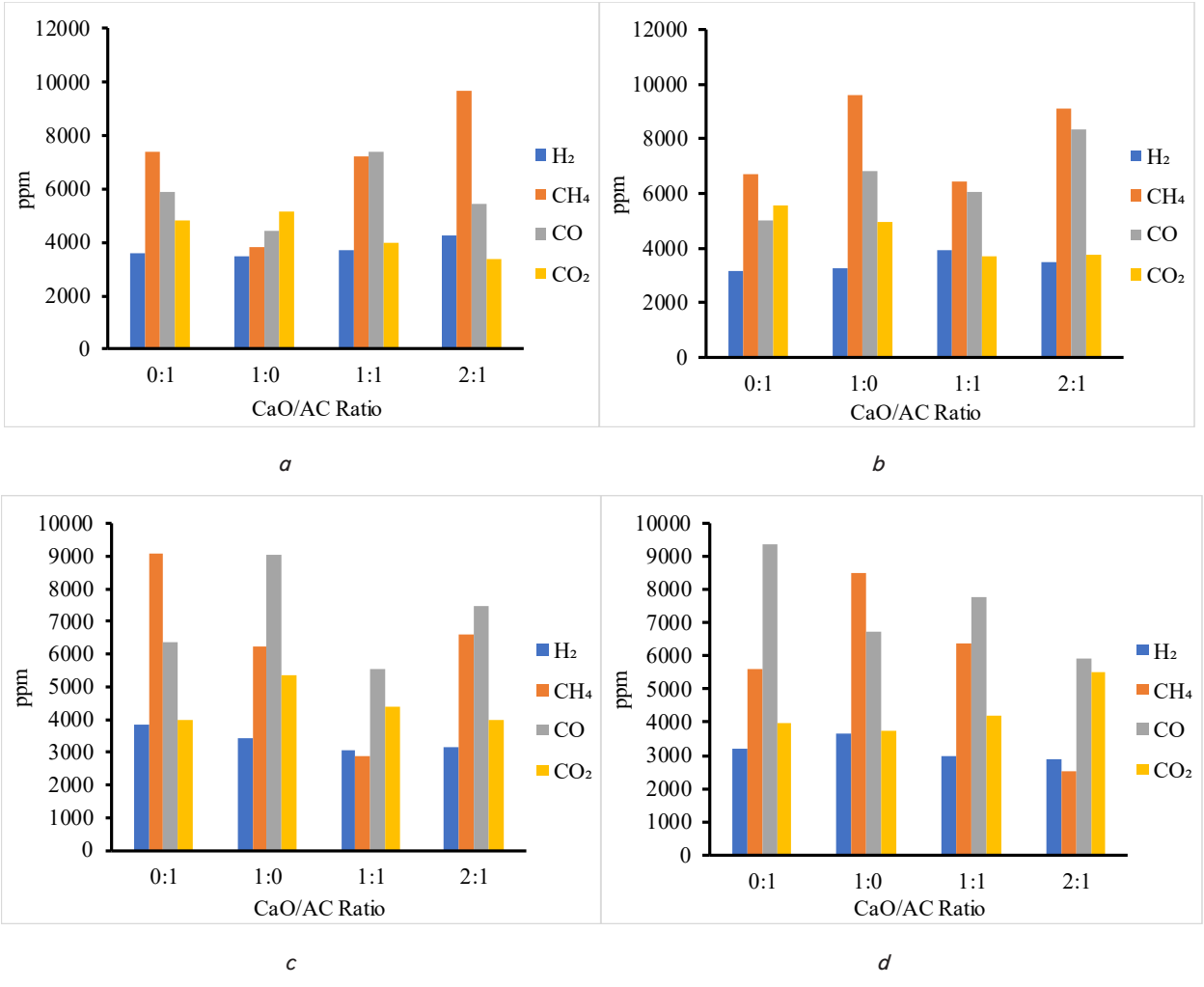

Fig. 7. Effect CaO/AC ratio with various catalyst load: *a* – 4%; *b* – 6%; *c* – 8%; *d* – 10%

5. 2. 4. Syngas low heating value

To calculate the LHV of syngas, it must first be converted from ppm to % volume of gas. The formula is $\%vol_i = \frac{ppmv_i}{10^4}$ to calculate the LHV:

$$LHV_{mix}\left(\frac{\text{MJ}}{\text{Nm}^3}\right) = \frac{10.8(\%\text{H}_2) + 12.63(\%\text{CO}) + 35.8(\%\text{CH}_4)}{100},$$

$LHV\ \text{H}_2 = 10.8\ \text{MJ/Nm}^3$,

$LHV\ \text{CO} = 12.63\ \text{MJ/Nm}^3$,

$LHV\ \text{CH}_4 = 35.8\ \text{MJ/Nm}^3$.

As shown in Fig. 8, the syngas low heating value (LHV) varies with the equivalence ratio (ER) and catalyst load.

Fig. 8 shows that the LHV value increases with the ER. At the same catalyst load of 4%, the LHV will increase in line with the increase in ER. ER 0.2 has the LHV of 230 kJ/kg and ER 0.35 has the LHV of 481 kJ/kg. Higher ER produces more intense autothermal conditions, causing the reactor temperature to rise. This increase in temperature accelerates the decomposition of volatiles and tar cracking, and promotes more complete gasification and reforming reactions, thereby increasing the fraction of permanent gases that contribute to the calorific value, mainly CO and CH_4, as well as some H_2. In addition, the increase in temperature is also associated with more effective hydrogen formation, because H_2 formation reactions (e.g., through steam-water and reforming reactions) are generally more optimal at high temperatures, with the temperature range often reported to be most conducive to H_2 formation being 800–1000°C.

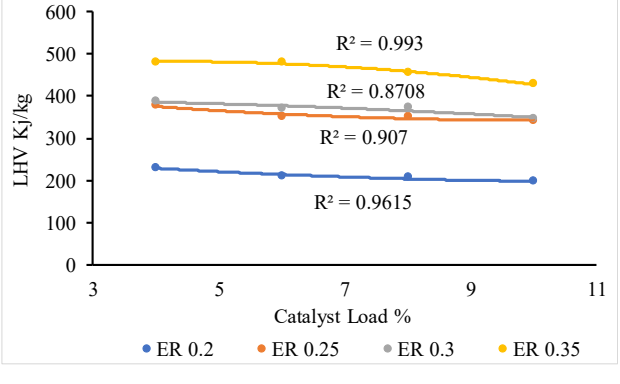

Fig. 8. Syngas low heating value with various equivalence ratio

At ER 0.2, the highest LHV was obtained at a catalyst load of 4% at 230 kJ/kg and continued to decrease with increasing catalyst load to 197 kJ/kg at 10%. At ER 0.25, the highest LHV was also obtained at a catalyst load of 4% at

377 kJ/kg and also decreased to 341 kJ/kg at a catalyst load of 10%. At ER 0.3, the highest LHV was obtained at a catalyst load of 4% at 388 kJ/kg and also decreased at a catalyst load of 10% to 347 kJ/kg. At ER 0.35, the highest LHV was obtained at 481 kJ/kg and decreased at a catalyst load of 10% to 428 kJ/kg.

However, all ER values show that LHV tends to decrease when the catalyst load is increased from 4% to 10%. This decrease indicates that excessive catalyst addition under these operating conditions does not always improve gas energy quality, because the catalyst can shift the reaction selectivity towards the conversion of high calorific components especially CH_4 into CO and H_2 through reforming, while at the same time the fraction of diluent gases such as CO_2 (and steam) may increase due to reaction. Since CH_4 has a very large calorific value contribution in the syngas mixture, the decrease in its fraction is often more dominant than the increase in CO/H_2, so that the total LHV tends to decrease.

In energy system analysis, particularly in combustion, gasification, and fuel gas utilization processes such as syngas, the LHV value is often used because it better represents the heat energy that can actually be utilized by the system. The LHV value of a fuel gas is usually influenced by the composition of combustible gases such as carbon monoxide (CO), hydrogen (H_2), and methane (CH_4). The higher the content of these gases, the greater the LHV value produced. The LHV of syngas from this study with variations in ER and CaO/AC-PF ratio can be seen in Fig. 9.

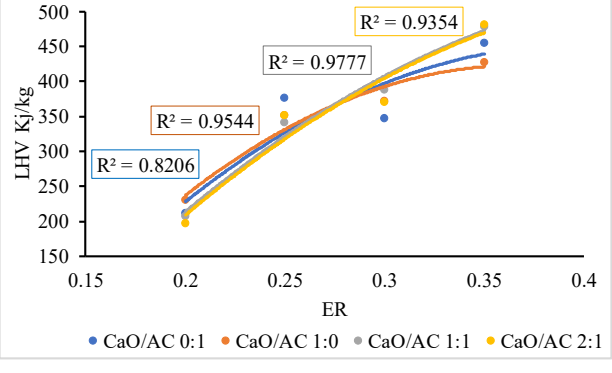

Fig. 9. Syngas low heating value with various CaO/AC ratio

Fig. 9 shows that the LHV of syngas increases consistently with the increase in ER 0.2 to 0.35 for all CaO/AC ratios, indicating that a higher ER strengthens autothermal conditions so that the reaction temperature increases and the conversion of volatiles into syngas becomes more complete. At low ER (0.2), the difference in LHV between ratios is still small because secondary reactions such as cracking, reforming and heterogeneous reactions are not yet dominant; the system is still relatively influenced by incompletely converted volatiles. When the ER is increased to 0.25–0.30, the effect of the catalyst ratio becomes apparent: compositions involving AC tend to produce higher LHV because they accelerate tar cracking and increase the fraction of calorific gas, while the contribution of CaO can shift the reaction equilibrium through a decrease in CO_2. At the highest ER (0.35), the LHV reaches its maximum at all ratios, with CaO/AC 2:1 and 0:1 showing peak values, indicating that at high temperatures, the reactive gas formation pathway (via cracking/reforming on the carbon surface and/or CaO-rich-promoted heterogeneous reactions) becomes dominant. Overall, ER acts as the main controlling factor for LHV increase through the temperature effect, while the CaO/AC ratio modulates LHV through the balance between cracking/reforming (AC) and CO_2 control (CaO), especially at medium-high ER.

6. Discussion on the catalytic effect of AC-PF/CaO and operating conditions on syngas composition and LHV

The interaction of the CaO-AC-PF catalyst to improve syngas quality can be seen from the characterization of the catalyst, the composition of the syngas and the LHV produced. From the scanning electron microscopy results in Fig. 2, it can be seen that the CaO:AC-PF;2:1 catalyst (Fig. 2, *c*) appears denser than the other catalysts. With the addition of CaO, CaO particle dispersion can be seen on the white carbon surface, indicating that some micro pores are closed by CaO. With the addition of CaO, a lot of CO_2 is absorbed and becomes $CaCO_3$. This porous structure is very important in top-flow gasification because pyrolysis gas and volatiles move through the layer, so the presence of a porous medium has the potential to strengthen secondary reactions and act as carbon capture before the gas exits to the condenser.

The interaction of the CaO-AC-PF catalyst in improving syngas quality can be observed from the catalyst characterization, syngas composition, and the resulting LHV. Based on the SEM results shown in Fig. 2, the CaO:AC-PF = 2:1 catalyst (Fig. 2, *c*) appears denser than the other catalyst formulations, indicating that CaO particles were dispersed on the carbon surface and may have partially blocked some of the smaller pores. This interpretation is reasonable because CaO-based materials are widely known to act as high-temperature CO_2 sorbents, and their carbonation proceeds through the formation of $CaCO_3$. During gasification, such sorption behavior can reduce CO_2 concentration and influence gas quality. In addition, porous carbonaceous media are known to promote tar cracking and secondary gas-phase reactions when volatile products pass through a hot solid bed. This is particularly relevant in fixed-bed gasification, where reactor design and the interaction between volatiles, char, and catalyst strongly affect tar conversion and gasification efficiency. Therefore, the porous structure of AC-PF, together with the CO_2-capturing role of CaO, may contribute to syngas upgrading before the gas exits the reactor system.

From a surface chemistry perspective, Fourier transform infrared spectroscopy (FTIR) shows the presence of -OH and calcium carbonate groups, as shown in Fig. 3. This is due to the results of KOH impregnation carried out during the manufacture of AC-PF. The presence of -OH groups functions as polar active sites capable of adsorbing polar molecules such as H_2O, CO_2, and volatile compounds. Surfaces with -OH groups tend to be hydrophilic and reactive, thereby enhancing interactions with tar compounds or heavy hydrocarbons. These tar compounds can then undergo thermal cracking or catalytic reforming into light gases such as H_2, CO, and CH_4. In addition to -OH, there are also O-H and C-O groups. The O-H group has characteristics that are almost the same as the -OH group, while the C-O group plays a role in enhancing the redox properties and chemical interactions between the carbon surface and gas molecules. In the gasification process, the C-O group can be part of the partial oxidation mechanism and carbon gasification reaction, which produces CO [25].

From a surface chemistry perspective, the Fourier transform infrared spectroscopy (FTIR) results indicate the presence of O-H, C-O, and carbonate-related groups, as shown in Fig. 3. The appearance of oxygen-containing functional groups is consistent with the use of KOH during the preparation of AC-PF, since KOH activation is known to modify the surface chemistry of activated carbon and promote the formation of oxygenated groups. O-H-containing groups can act as polar active sites that enhance the interaction of the carbon surface with polar molecules such as H_2O, CO_2, and oxygenated volatile compounds. Such surface functionality may also facilitate the adsorption of tar-related species and support their further conversion through thermal cracking or reforming into lighter gases. In addition to O-H groups, the presence of C-O groups suggests that the carbon surface retains oxygen-containing functionalities that may contribute to surface reactivity and gas-solid interactions. During gasification, these surface groups may participate indirectly in oxidation-reduction interactions at the carbon surface and support the formation of combustible gases such as CO. The carbonate-related bands may also indicate the presence of calcium-containing carbonate species, which is consistent with the CO_2-capturing function of CaO during the gasification process.

The BET data in Fig. 4 shows that the surface area decreased to 5.06 m^2/g, but the pore diameter increased to a mesopore scale of 22.87 nm, which can improve the accessibility of volatiles to active sites and improve mass transport in the reforming reaction. In Fig. 4, *b*, the BJH curve at CaO:AC-PF = 2:1 shows the highest *dV/dD* values of 30–40 nm, indicating a catalyst in the mesopore size range. The presence of these mesopores will further increase the active sites for CO_2 adsorption.

The BET results presented in Fig. 4 show that the specific surface area decreased to 5.06 m^2/g, while the average pore diameter increased to 22.87 nm, corresponding to the mesopore range. This change suggests that, although the surface area became lower, the larger pore structure may improve the accessibility of volatile compounds to active sites and enhance mass transport during reforming reactions. In Fig. 4, *b*, the BJH pore size distribution of the CaO:AC-PF = 2:1 catalyst shows the highest *dV/dD* values in the pore diameter range of 30–40 nm, confirming the dominance of mesopores in this catalyst. The presence of these mesopores may facilitate gas diffusion and improve contact between gaseous species and the catalyst surface, which can contribute to CO_2 adsorption and syngas upgrading during gasification.

From a process perspective, in Fig. 5, ER appears as the dominant variable that regulates autothermal conditions, primarily through an increase in effective temperature and secondary reaction intensity. An increase in ER from low to high levels consistently increases H_2, which can be explained by the acceleration of H_2 formation reactions such as charcoal gasification with steam ($C + H_2O \rightarrow CO + H_2$) [26], light hydrocarbon reforming, and more intense tar cracking at high temperatures. At the same time, CH_4 also increases sharply at high ER, indicating that in an autothermal upflow system, increased temperature and changes in gas composition can facilitate the formation of light gases. Meanwhile, CO tends to peak at moderate ER and then decreases at high ER, consistent with competition between CO formation and CO consumption through subsequent reactions such as methanation [27]. The decrease in CO_2 at high ER indicates the role of high temperatures in enhancing the reduction of CO_2 by charcoal (Boudouard reaction) and/or the role of CaO adsorption if available.

The effect of catalyst loading in Fig. 6 shows that adding catalyst does not always increase H_2. Increasing the catalyst loading from low to high tends to reduce H_2 and CH_4 but increase CO. Mechanistically, this condition can occur when the catalyst strengthens pathways that increase CO and/or promotes RWGS ($CO_2 + H_2 \rightarrow CO + H_2O$) [28], which consumes H_2 so that net H_2 is reduced. Furthermore, at high catalyst loadings, the possibility of diffusion/aggregation penalties increases, so that selectivity may shift and some active sites become less effective. Therefore, the target of H_2-rich synthesis gas in this reactor is more dependent on ER adjustment and the selection of moderate/low catalyst loadings, rather than simply increasing the loading.

The CaO/AC-PF ratio in Fig. 7 shows synergistic but non-linear behavior. AC-PF plays a major role as a porous medium that enhances the cracking/reforming process of volatile compounds, while CaO provides a basic site and CO_2 absorber to shift the equilibrium. At high CaO ratios, sorption and base effects may increase, but the risk of micro-pore closure and diffusion pathway changes also increases. This explains why certain compositions are optimal at certain catalyst loads: the best performance arises from a balance between pore accessibility (the role of AC-PF) and sorption/base strength (the role of CaO).

From an energy quality perspective in Fig. 8, 9, the LHV value of synthetic gas is highly sensitive to changes in CH_4. Therefore, high ER conditions that increase CH_4 tend to increase LHV. H_2, CH_4 and CO are the main factors for obtaining high LHV. CO_2 has no calorific value so it must be captured. In this study, CaO was used so that CO_2 could be suppressed, meaning that the total LHV could be increased. The highest LHV in this study was 481 kJ/kg, while in another study, the highest was 550 kJ/kg using pinewood with dolomite, activated carbon, silica gel, and limestone catalysts [29]. The higher the ER, the more oxygen enters the system, thereby increasing the reforming reaction [30].

In comparison with the literature reviewed in this study, the present study demonstrates a comparable qualitative trend, particularly in showing that catalyst-assisted updraft gasification can improve syngas composition and energy quality. For example, previous studies reported that dolomite-assisted rice husk gasification increased H_2 content up to 15.4 mol% with an LHV of 5.1 MJ/Nm^3, while other updraft gasification systems with catalytic enhancement also showed improved hydrogen-rich syngas production and higher heating values. In the present study, the highest syngas LHV reached 481 kJ/kg under the investigated conditions, indicating that the CaO/AC-PF catalyst system was effective in improving gas quality, although the absolute value remains influenced by the use of corncob feedstock, the small-scale reactor design, and the sensor-based gas measurement approach. Therefore, the present results support the view that the combined CaO/AC-PF catalyst is a promising low-cost alternative for syngas upgrading, particularly for agricultural biomass gasification in simple updraft systems.

In practical terms, the present study is relevant to the development of low-cost biomass gasification systems that can utilize locally available agricultural residues and catalyst materials. Corncob is a commonly available agricultural by-product; while CaO and activated carbon are obtained from palm-fiber waste, which can be sourced at relatively low-cost. Thus, the suggested catalyst system may have prac-

tical application in small-scale updraft gasifiers operating on agricultural residues where low-cost waste-to-energy technologies are needed. The syngas generated from that sort of systems may be used straight like a combustible gas for thermal functions, akin to drying or heating or in energy generation on a small scale; Its potential as an intermediate gas for additional upgrading/conversion into different value-added vitality and chemical substances is notable.

There are some limitations in this study. First, the gas written is based on ppm taken from an MQ sensor, thus, there could be a minor effect (relative accuracy) by cross-sensitivity and limitations of the humidity in addition to possible drift and temperature during gas capture; one entry point that can influence the %vol estimation and consequently affect LHV calculation whenever variations in CO and CH_4 occurs homogeneously. Second, the catalyst characterization (SEM-FTIR-BET) confirms the importance of surface structure and composition, but has not quantified alterations in the active phase under reaction conditions, extent of carbonation and gradual loss of activity due to pore blocking build-up.

The drawback of this study is that CaO catalyst is quite reactive with CO_2. Calcium oxide [CaO] (obtained from the calcination process) has to be kept in a closed space so that it does not form calcium carbonate $CaCO_3$. Because the catalyst is covered with tar or ash, it has a limited lifetime.

Hence, some future directions are suggested based on these limitations. It is better to use GC-TCD/GC-FID to calibrate the gas composition so that it is possible to report the sensor readings as more accurate %vol include LHV uncertainty analysis. Catalyst stability and possibility for regeneration, particularly with respect to the highly carbonatable CaO species, can be evaluated using carbonation-calcination cycle tests combined with post-reaction characterization (XRD/TGA/SEM-EDX) to assess phase alterations and loss of activity. Design experiments directed at ANOVA or RSM interactions such that interaction effects can be obtained and predictive models confirmed by replication confirmation tests. Include process performance metrics such as gas yield (Nm^3/kg), cold gas efficiency, pressure drop and air consumption so that syngas quality improvement can be shown on the basis of mass-energy balance and operability and not only composition.

7. Conclusion

1. The current study indicated that the CaO/AC-PF catalyst system can significantly enhance syngas quality for corncob updraft gasification. Characterization of the catalyst using SEM, FTIR and BET revealed that the resulting combined catalyst possessed altered surface morphology, oxygen-functional groups, carbonate counterpart species and meso-porous traits; CaO:AC-PF = 2:1 boasted a specific area of 5.06 m^2/g and pore average diameter 22.87 nm. These properties suggest that changes in the catalyst structure occurred, which might aid gas–solid interaction during gasification.

2. Equivalence ratio, catalyst loading, and CaO/AC ratio affected syngas composition and heating value in the gasification experiments. From ER 0.20 to 0.35, the H_2 concentration increased from 3150 to 3914 ppm; the CH_4 concentration increased from 3093 to 9221 ppm and the syngas LHV was elevated from 230 to 481 kJ/Nm^3. For catalyst loading, by enhancing the loading from 4 wt. % to 10 wt. With 30% for H_2, CH_4 was reduced from 3742 to 3176 ppm and 7031 to 5746 ppm, while CO increased (5783 to7445 ppm). These findings suggest that the quality of syngas was influenced by competition between catalytic activity, pore accessibility and behavior concerning sorption of CO_2.

Conflict of interest

The authors declare that they have no conflict of interest in relation to this study, whether financial, personal, authorship or otherwise, that could affect the study and its results presented in this paper.

Financing

The authors sincerely thank the Ministry of Education, Culture, Research and Technology, Republic of Indonesia for fully supporting this study through the DRTPM Research Grant under Fundamental Research, Universitas Widyagama Malang, Indonesia 2025 (Grant Number:128/C3/DT.05.00/PL/2025;023/LL7/DT.05.00/PL/2025;010/ Kontrak/PT/PTS.030.7/PN/V/2025).

Data availability

Manuscript has no associated data.

Use of artificial intelligence

The authors used the AI-based language model ChatGPT (GPT-5.3) only to assist in improving the clarity of English language and grammar in several sections of the manuscript, particularly in the Introduction and Literature Review sections.

The AI tool was used solely for language editing and paraphrasing purposes. All scientific content, experimental design, data analysis, and interpretation of the results were conducted entirely by the authors.

The authors carefully reviewed and verified all AI-assisted text to ensure accuracy and consistency with the experimental results. The use of AI tools did not influence the scientific conclusions of this study.

Acknowledgements

We as the Research Team would like to thank Ministry of Education, Culture, Research and Technology, Republic of Indonesia (Kemendiktisaintek Indonesia) for financing research activities.

Authors' contributions

Purbo Suwandono: Conceptualization, Writing-original draft, Investigation, Supervision, Formal analysis, Writing – review & editing; **Widya Wijayanti**: Validation, Investigation, Data Curation, Formal analysis, Writing – original draft; **Nova Risdiyanto Ismail**: Writing – review & editing, Formal analysis; **Dzulfikar Johan Akbar:** Visualization, Writing – original draft, Data curation; **Muhammad Reza**: Project administration, Resources, Data curation.

References

1. Yadav, V. K., Sharma, A. K., Gacem, A., Pandit, J., Wany, A., Kumar, A. et al. (2025). Emerging Trends in the Valorization of Agricultural Waste and Their Utilization in Agricultural, Pharmaceuticals, and Environmental Cleanup. Waste and Biomass Valorization, 16 (6), 2779–2833. https://doi.org/10.1007/s12649-025-03002-y
2. Lewandowski, W. M., Ryms, M., Kosakowski, W. (2020). Thermal Biomass Conversion: A Review. Processes, 8 (5), 516. https://doi.org/10.3390/pr8050516
3. Ariyanti, D., Rimantho, D., Leonardus, M., Ardyani, T., Lisnawati, Fiviyanti, S. et al. (2025). Valorization of corn cob waste for furfural production: A circular economy approach. Biomass and Bioenergy, 194, 107665. https://doi.org/10.1016/j.biombioe.2025.107665
4. Zhang, J., Chu, Z., Cao, R., Wu, X., Han, K. (2026). A review of resource recovery from waste plastics via pyrolysis and gasification. Fuel, 404, 136319. https://doi.org/10.1016/j.fuel.2025.136319
5. Tangke Tosuli, Y., Cahyadi, Dafiqurrohman, H., Hermawan, R., Surjosatyo, A. (2024). Gasification of sago dreg waste in a top-lit updraft fixed bed gasifier: Syngas composition and its effect with additional Al2O3 as catalyst. Energy Conversion and Management: X, 24, 100775. https://doi.org/10.1016/j.ecmx.2024.100775
6. Tuan, P. D., Minh Quan, L., Nhi, V. T., Huong, H. M., Phung, L. T. K., Feng, D. (2022). Enrichment of hydrogen in product gas from a pilot-scale rice husk updraft gasification system. Carbon Resources Conversion, 5 (3), 231–239. https://doi.org/10.1016/j.crcon.2022.07.003
7. Yousef, S., Eimontas, J., Zakarauskas, K., Striūgas, N. (2025). Oxygen updraft gasification-catalytic reforming of cigarettes butts for hydrogen-rich syngas production. International Journal of Hydrogen Energy, 171, 150650. https://doi.org/10.1016/j.ijhydene.2025.150650
8. Bilbao, D. C., Machin, E. B., Pedroso, D. T., Hernández, D., Aburto-Hole, J., Muñoz, L. (2025). Experimental assessment of the energy potential of pellets produced from beekeeping wastes by updraft gasification. Energy Conversion and Management, 343, 120206. https://doi.org/10.1016/j.enconman.2025.120206
9. Yesilova, N., Tezer, O., Ongen, A., Ayol, A. (2024). Enhancing biomass gasification: A comparative study of catalyst applications in updraft and modifiable-downdraft fixed bed reactors. International Journal of Hydrogen Energy, 76, 290–303. https://doi.org/10.1016/j.ijhydene.2024.05.075
10. Jančauskas, A., Striūgas, N., Zakarauskas, K., Skvorčinskienė, R., Eimontas, J., Buinevičius, K. (2024). Experimental investigation of sorted municipal solid wastes producer gas composition in an updraft fixed bed gasifier. Energy, 289, 130063. https://doi.org/10.1016/j.energy.2023.130063
11. Junga, R., Tańczuk, M., Sobek, S., Chabiński, M., Ziółkowski, Ł., Werle, S. (2023). Effect of the addition of laying hens manure to the straw on gasification efficiency in updraft gasifier under air atmosphere. Applied Thermal Engineering, 226, 120269. https://doi.org/10.1016/j.applthermaleng.2023.120269
12. Tezer, Ö., Karabağ, N., Öngen, A., Ayol, A. (2023). Gasification performance of olive pomace in updraft and downdraft fixed bed reactors. International Journal of Hydrogen Energy, 48 (60), 22909–22920. https://doi.org/10.1016/j.ijhydene.2023.02.088
13. Işık, K. E., Dogru, M., Erdem, A. (2023). Gasification of MDF residue in an updraft fixed bed gasifier to produce heat and power via an ORC turbine. Waste Management, 169, 43–51. https://doi.org/10.1016/j.wasman.2023.06.025
14. Gorthy, S., Verma, S., Sinha, N., Shetty, S., Nguyen, H., Neurock, M. (2023). Theoretical Insights into the Effects of KOH Concentration and the Role of OH– in the Electrocatalytic Reduction of CO2 on Au. ACS Catalysis, 13 (19), 12924–12940. https://doi.org/10.1021/acscatal.2c06115
15. Wang, X., Zeng, W., Xin, C., Kong, X., Hu, X., Guo, Q. (2022). The development of activated carbon from corncob for CO2 capture. RSC Advances, 12 (51), 33069–33078. https://doi.org/10.1039/d2ra05979g
16. Zhou, B., Bai, B., Zhu, X., Guo, J., Wang, Y., Chen, J. et al. (2024). Insights into effects of grain boundary engineering in composite metal oxide catalysts for improving catalytic performance. Journal of Colloid and Interface Science, 653, 1177–1187. https://doi.org/10.1016/j.jcis.2023.09.148
17. Zhu, Y., Wu, J., Zhang, Y., Miao, Z., Niu, Y., Guo, F., Xi, Y. (2024). Preparation of hierarchically porous carbon ash composite material from fine slag of coal gasification and ash slag of biomass combustion for CO2 capture. Separation and Purification Technology, 330, 125452. https://doi.org/10.1016/j.seppur.2023.125452
18. Ilić, M., Haegel, F.-H., Lolić, A., Nedić, Z., Tosti, T., Ignjatović, I. S. et al. (2022). Surface functional groups and degree of carbonization of selected chars from different processes and feedstock. PLOS ONE, 17 (11), e0277365. https://doi.org/10.1371/journal.pone.0277365
19. Ali, R., Aslam, Z., Shawabkeh, R. A., Asghar, A., Hussein, I. A. (2020). BET, FTIR, and RAMAN characterizations of activated carbon from wasteoil fly ash. Turkish Journal of Chemistry, 44 (2), 279–295. https://doi.org/10.3906/kim-1909-20
20. Stanienda-Pilecki, K. J. (2019). The importance of Fourier-Transform Infrared Spectroscopy in the identification of carbonate phases differentiated in magnesium content. Spectroscopy, 34 (6). Available at: https://www.spectroscopyonline.com/view/spec0619-pilecki
21. Dai, F., Zhuang, Q., Huang, G., Deng, H., Zhang, X. (2023). Infrared Spectrum Characteristics and Quantification of OH Groups in Coal. ACS Omega, 8 (19), 17064–17076. https://doi.org/10.1021/acsomega.3c01336
22. Martínez de Salazar Martínez, E., Alexandre-Franco, M. F., Nieto-Sánchez, A. J., Cuerda-Correa, E. M. (2024). Exploring the role of surface and porosity in CO2 capture by CaO-based adsorbents through response surface methodology (RSM) and artificial neural networks (ANN). Journal of CO2 Utilization, 83, 102773. https://doi.org/10.1016/j.jcou.2024.102773

23. Tavizón-Pozos, J. A., Cervantes-Cuevas, H., Garcia-Camacho, G. G., Chavez-Esquivel, G., Acosta-Najarro, D. R. (2025). Biodiesel Production Using K–Sr/CaO and CaO Catalysts Derived from Eggshells by Canola Oil Transesterification. ACS Omega, 10 (7), 6827–6838. https://doi.org/10.1021/acsomega.4c09118
24. Koo-amornpattana, W., Phadungbut, P., Kunthakudee, N., Jonglertjunya, W., Ratchahat, S., Hunsom, M. (2023). Innovative metal oxides (CaO, SrO, MgO) impregnated waste-derived activated carbon for biohydrogen purification. Scientific Reports, 13 (1). https://doi.org/10.1038/s41598-023-31723-4
25. Quan, C., Wang, M., Gao, N., Yang, T., Li, R. (2023). In situ adsorption of CO2 to enhance biomass gasification for hydrogen production using Ca/Ni based composites. Journal of the Energy Institute, 108, 101229. https://doi.org/10.1016/j.joei.2023.101229
26. Micheli, F., Mattucci, E., Courson, C., Gallucci, K. (2021). Bi-Functional Catalyst/Sorbent for a H2-Rich Gas from Biomass Gasification. Processes, 9 (7), 1249. https://doi.org/10.3390/pr9071249
27. Zhu, M., Wang, Q., Wang, S. (2025). Recent Advances and Future Perspectives in Catalyst Development for Efficient and Sustainable Biomass Gasification: A Comprehensive Review. Sustainability, 17 (16), 7370. https://doi.org/10.3390/su17167370
28. Cerone, N., Zimbardi, F., Contuzzi, L., Baleta, J., Cerinski, D., Skvorčinskienė, R. (2020). Experimental investigation of syngas composition variation along updraft fixed bed gasifier. Energy Conversion and Management, 221, 113116. https://doi.org/10.1016/j.enconman.2020.113116
29. Mohanty, R., Mahanta, P., Mahapatro, A., Sharma, R. P. (2025). Catalytic gasification of pinewood biomass in a fluidized bed reactor with dolomite, limestone, and activated carbon: An experimental study. Energy, 325, 136131. https://doi.org/10.1016/j.energy.2025.136131
30. Liu, C., Huang, Y., Niu, M., Pei, H., Liu, L., Wang, Y. et al. (2018). Influences of equivalence ratio, oxygen concentration and fluidization velocity on the characteristics of oxygen-enriched gasification products from biomass in a pilot-scale fluidized bed. International Journal of Hydrogen Energy, 43(31), 14214–14225. https://doi.org/10.1016/j.ijhydene.2018.05.154